Heliyon 11 (2025) e42095

Contents lists available at ScienceDirect

Heliyon

journal homepage: www.cell.com/heliyon

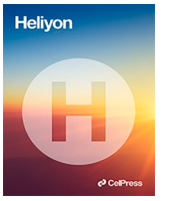

Research article

Dihydroartemisinin inhibits EphA2/PI3K/Akt pathway-mediated malignant behaviors and vasculogenic mimicry in glioma stem cells

Huangde Fu [a,b,1,*], Shengtian Wu [a,1], Hechun Shen [a], Kai Luo [a], Zhongxiang Huang [c], Nankun Lu [a], Yaolin Li [a], Qian Lan [d], Yishun Xian [a]

[a] Department of Neurosurgery, The Second Nanning People's Hospital, Guangxi, China
[b] Department of Neurosurgery, The Third Nanning People's Hospital, Guangxi, China
[c] Department of Pathology, The Second Nanning People's Hospital, Guangxi, China
[d] Department of Clinical Laboratory, The Second Nanning People's Hospital, Guangxi, China

ARTICLE INFO

Keywords:
Dihydroartemisinin
EphA2
Glioma
Malignant behaviors
Vasculogenic mimicry

ABSTRACT

Gliomas, the most prevalent primary brain tumors, exhibit a poor five-year survival rate despite advances in various treatments, necessitating further studies to understand tumor progression and develop new therapies, particularly targeting EphA2, which is implicated in vasculogenic mimicry and glioma progression. Dihydroartemisinin (DHA) has shown anti-glioma effects through mechanisms such as PERK-related ferroptosis and inhibition of proliferation and angiogenesis, although its interaction with EphA2 in mediating these effects requires further investigation. In this study, we revealed that DHA significantly inhibits the formation of vasculogenic-like networks, the stemness of C6 glioma stem cells and the growth of glioma by inhibiting the expression of EphA2. Mechanistic investigations indicated that PI3K/Akt pathway at least partly mediated this function, since overexpression of EphA2 reversed the anti-tumor effects of DHA. Conclusively, the current report provides evidence that DHA, PI3K/Akt/EphA2 blockage, and VM inhibition are promising therapies for glioma.

1. Introduction

As the most common primary brain tumor in both children and adults, glioma accounts for 7 % of cancer-related death before the age of 70 years [1,2]. Despite recent advances in treatment for glioma patients, including surgical resection, radiotherapy, chemotherapy and immunotherapy, patients with newly diagnosed glioblastoma exhibit an unsatisfactory five-year survival rate (4.7 %) [1,3]. Anti-angiogenic therapy, which is commonly used as an adjunct in clinical settings due to the hypervascular neoplasia nature of GBM, has its limitations [4]. Therefore, more mechanistic studies providing insights of tumor occurrence and progression and developing novel therapies are urgently required. Manitotis et al. reported a phenomenon termed as vasculogenic mimicry (VM), which refers to a novel paravascular tumor blood supply pattern in highly aggressive uveal melanomas. This pattern is formed by tumor cells rather than endothelial cells [5]. VM, which is characterized by microvascular channels formed by tumor cells, acts as an

* Corresponding author. Department of Neurosurgery, The Second Nanning People's Hospital, Guangxi, China.
E-mail address: qt000172@sr.gxmu.edu.cn (H. Fu).
[1] These authors contribute equally to this work.

https://doi.org/10.1016/j.heliyon.2025.e42095
Received 13 May 2024; Received in revised form 15 January 2025; Accepted 17 January 2025
Available online 20 January 2025

alternative oxygen and nutrient supply route for these cells, and is considered to be associated with tumor progression and poor clinical prognosis in preclinical models and patients [6]. Recently, experimental evidence has shown the roles of several key regulators in the formation of VM by melanoma cells, including Eph receptor A2 (EphA2), a member of the largest receptor tyrosine kinase subfamily [7]. EphA2 has been recognized as a mitogen in the development of glioma. It is reported that targeting EphA2 also reduces glioblastoma stemness, suppresses tumor growth and could potentially improve survival of patients [8–10]. Phosphoinositide 3 kinase (PI3K)/Akt/matrix metalloproteinases (MMP) 2/9 signalling was considered another essential pathway mediating EphA2-related VM formation [8–10].

Dihydroartemisinin (DHA), a main active derivative of artemisinin which acts as the active principle of Artemisia annua L [11], has been revealed to exert preferentially cytotoxic effects toward several malignancies such as lung [12], breast [13] and colorectal cancer [14]. Chen et al. demonstrated that DHA exerts anti-glioma effects, at least partly mediated by protein kinase R-like ER kinase (PERK)-related ferroptosis [15] and extrachromosomal DNA-dependent epithelial-mesenchymal transition (EMT) [16]. Other mechanisms underlying the antitumor effects include inhibition of proliferation and angiogenesis, and induction of autophagy, endoplasmic reticulum and apoptosis [17]. However, whether EphA2 mediates the anti-VM and anti-glioma effects of DHA remains unclear.

In this study, we aim to elucidate the potential role of the DHA treatment and knockdown of EphA2 in shaping VM formation in C6-brain glioma stem cells (BGSCs). These research provided novel mechanistic understanding and preclinical evidence for the administration of DHA and inhibition of EphA2 in the treatment of glioma.

2. Materials and methods

2.1. Drugs

DHA was purchased from Company Chemsrc (Shanghai, China). PI3K inhibitor LY294002 was purchased from Beyotime Institute of Biotechnology (Shanghai, China) and stored at −20 °C.

2.2. Cell culture

C6 Glioma cell lines purchased from China Center for Type Culture Collection (CCTCC) were cultured in DMEM (Gibco, NY, USA) containing 10 % fetal bovine serum (FBS, Gibco, Australia), 1 % penicillin/streptomycin (Cat# 15070-063, Gibco, USA) and aseptically grown at 37 °C in a humidified incubator containing 5 % CO_2. The culture medium was replaced after 5 days. After 10 days, digestion and centrifugation were performed, and then the cells were re - inoculated into DMEM/F12 serum - free medium. After the glioma cell clonal spheres had been passaged for 3 times, the cell monoclonal culture experiment was conducted on the 3rd-generation C6-BGSCs. Dynamically observed the division of single cells and the formation of clones in the marked wells every day. After about one week of culture, observed and collected the clonally proliferated cells under an inverted microscope, transferred them to culture flasks for continuous culture and amplification, so as to obtain a large number of subcell line clonal spheres derived from the same cell. The cells that had undergone clone screening and purification were used for the next research step and were called stem cells. Glioma stem cells were incubated with DMEM/F12 serum-free medium (containing 20 μg/L epidermal growth factor, 10 μg/L fibroblast growth factor, 2 % B27) at a density of 2×10^5 and cultured in an incubator with 5 % CO_2 at 37 °C. After 5 days, the medium was changed. After 10 days, the glioma cells were digested, centrifuged, and re-incubated into serum-free DMEM/F12. The glioma cells were considered to be glioma stem cells after 3 times of clonal ball passage, which was further identified by assessing the expression of CD133 (Supplementary Figs. 1A and B).

2.3. Cell viability assay

The cell viability of C6 and C6-BGSC under different treatment conditions was measured using the Cell Counting Kit-8 (CCK-8) cell counting kit (C0037,Beyotime, China). Cells were resuspended, counted, and plated at approximately 4000 cells/well in a 96-well plate, and treated with different concentrations of DHA (0, 10, 25, 50, 75, 100, 200 μM) for up to 24h, 48h, 72h or concentrations of 100 μM DHA treated for 6 h, 12 h, 24h and 48 h. Subsequently, 15 μL of CCK-8 solution was added to each well, and the cells were cultured for another 2 h. The optical density of cells was measured at a wavelength of 450 nm using a microplate reader (Multiskan FC, Thermo Scientific, United States).

2.4. Flow cytometry analysis of apoptosis

For apoptosis analysis, BGSCs were treated with 100 μM DHA or DMSO for 48 h, combined with or without siEphA2, pc-EphA2 or LY294002 (50 nM). the cells then were collected and centrifuged after trypsinization without EDTA, and washed twice with cold PBS. According to the manufacturer's recommendations, the pelleted cells were resuspended in 300 μL Binding Buffer, and 5 μL Annexin V-FITC and 10 μL PI staining solution (Annexin V-FITC/PI apoptosis kit; 401003,BestBio, China) were added and stained under light for 5 min. The percentage of apoptotic cells was assessed using flow cytometry analyzed using FlowJo software.

2.5. Western blotting

Cells were lysed by pre-cooled RIPA lysis buffer (Solarbio, China) with PMSF(Solarbio, China) on ice for 30 min, followed by

centrifugation at 13 000×*g* for 15 min at 4 °C. Protein was quantified with the bicinchoninic acid (BCA) quantification kit.

Loading buffer-mixed protein samples were subsequently boiled and separated using electrophoresis and transferred to nitrocellulose membranes (10600003,Cytiva, Life Sciences). The membrane was blocked in TBST containing 5 % skim milk for 2 h, incubated with primary antibodies including rabbit anti-CD133 (1:2000, ab284389, abcam), rabbit anti-MMP2 (1:2000, 10373-2-AP, proteintech), rabbit anti-MMP3 (1:3000, 17873-1-AP, proteintech), rabbit anti-MMP9 (1:2000, 27306-1-AP, proteintech), rabbit anti-Bcl-2 (1:2000, 12789-1-AP, proteintech), rabbit anti-Bax (1:2000, 50599-2-Ig, proteintech), rabbit anti-EphA2 (1:2000, bs-10209R, bioss), rabbit anti-AKT (1:2000,60203-2-Ig, proteintech), rabbit anti-p-AKT (1:1000, 80455-1-RR, proteintech), rabbit anti-PI3K (1:2000, ab227204, abcam), rabbit anti-p-PI3K (1:1000, ab182651,abcam) overnight at 4 °C. Membranes were washed three times with TBST, and incubated with horseradish peroxidase (HRP)-conjugated secondary antibodies for 1 h. After washing the membrane three times with TBST, blots were detected using the Super Sensitive ECL-solution (ECL-0011, Dingguo, China) on a ChemiScope 5300 Pro intelligent image workstation (Clinx, China) and analyzed using ImageJ.

2.6. Tube-formation assay

For the in vitro tube formation assay, basement membrane matrigel(#356234, Corning,USA) was applied to a 24-well tissue culture plate (200 μl per well). After polymerization of the matrigel at 37 °C for 1 h, cells starved for 2 h were harvested using trypsin/EDTA, washed with assay medium, and seeded at a density of 1×10^5 cells per well on the polymerized matrigel in the presence of different formulations (i.e. DHA [at 100 μM] or DMSO). The medium containing no DHA was set as the control, and the medium containing 30 ng/ml VEGF was set as the positive control. After being shaken for 15 s with orbital shaker, the plate was kept in the cell incubator for 24 h. Representative pictures of tube formation were taken at 10 × magnification under a stereomicroscope (Olympus, IX71, Japan) and tubes were counted for statistical analysis (n = 4).

2.7. Immunofluorescent staining(IF staining)

Cells were seeded in a 24-well plate with cell coverslips at a density of 30000 cells/well. The cells were treated with 100 μM DHA or DMSO for 24h. The cells were rinsed once with PBS, fixed with 4 % paraformaldehyde for 20 min, and then washed with PBS three times for 5 min each. After that, the plates were blocked and permeabilized with 0.1 % Triton X-100 in PBS containing 5 % bovine serum albumin (BSA) at room temperature for 1 h. Subsequently, cells were incubated with primary antibody overnight at 4 °C, including rabbit anti-EphA2 (1:500, #14074, CST), rabbit anti-MMP2 (1:500, #9661, CST). Then, cells were washed with PBS three times for 5 min each, and incubated with secondary antibody at 1:500 for 1 h at room temperature. After rinsing three more times with PBS, Hoechst 33342 was stained (62249,Thermo Fisher Scientific) for 10 min at 1:10000 and then coverslips were mounted the slides with an anti-fluorescence decay mounting medium. Images were acquired by confocal (Olympus, Japan) and ImageJ software was used for analysis.

2.8. si-RNAs, plasmids and cell transfection

Cells were seeded in 6-well or 96-well plates at a density of 5×10^3 cells/well or 1.5×10^5 cells/well, respectively, and transfected with a serum-free medium containing Lipofectamine 3000™ Transfection Reagent (L3000-015, InvitrogenTM) for 100 pmol si-NC or si-EpaA2 for 6 h according to the manufacturer's instruction. The transfection efficiency peaked at 72 h, and subsequent experiments were carried out. The primer sequences of si-EpaA2 and pc-EpaA2 are listed in Table 1.

2.9. RNA extraction and quantitative real-time PCR

Total RNA was extracted from cells using RNA extraction method based on Trizol (No.20211125, invitrogen). RNA (500 ng) was reverse transcribed into single-stranded cDNA using Revert Aid First Strand cDNA Synthesis Kit(K1622, Thermo Fisher Scientific) according to the protocol provided by the manufacturer. PCR amplification of target cDNA and internal control (GAPDH) cDNA was performed using specific primers. Sample mRNA levels were quantified using DyNAmo Flash SYBR Green qPCR Kit (F-415XL, Thermo

Table 1
Sequences of primers and siRNAs.

Name	Sequence(5′-3′)	Sequence(5′-3′)	Trials
CD133	Forward: CTGCCCAGAGTGGAAGAAT	Reverse: ACAGCAAGCCCAGGTAAAA	qPCR
MMP2	Forward: TAACTCCACTACGCTTTT	Reverse: TACTTTACTCGGACCACT	qPCR
MMP3	Forward: CCCTGATGTCCTCGTGGTA	Reverse: GGTCCTGAGAGATTTTCGC	qPCR
MMP4	Forward: CCCTGATGTCCTCGTGGTA	Reverse: GGTCCTGAGAGATTTTCGC	qPCR
MMP9	Forward: TGAAGACGACATAAAAGGCA	Reverse: GGGACACATAGTGGGAGGAG	qPCR
EphA2	Forward: TGTGTGGCATTGCTCTCT	Reverse: TTCTCGTAGCCTTCTTGG	qPCR
GAPDH	Forward: ACAGCAACAGGGTGGTGGAC	Reverse: TTTGAGGGTGCAGCGAACTT	qPCR
Epha2-rat-1385	Sense:GGAAGUACGAAGUCACCUATT	Anti-sense:UAGGUGACUUCGUACUUCCTT	Gene silencing
Epha2-rat-2023	Sense:GGCGUUGUCUCUAAAUACATT	Anti-sense:UGUAUUUAGAGACAACGCCTT	Gene silencing
Epha2-rat-1715	Sense:CCAAGUCAGAACAACUAAATT	Anti-sense:UUUAGUUGUUCUGACUUGGTT	Gene silencing

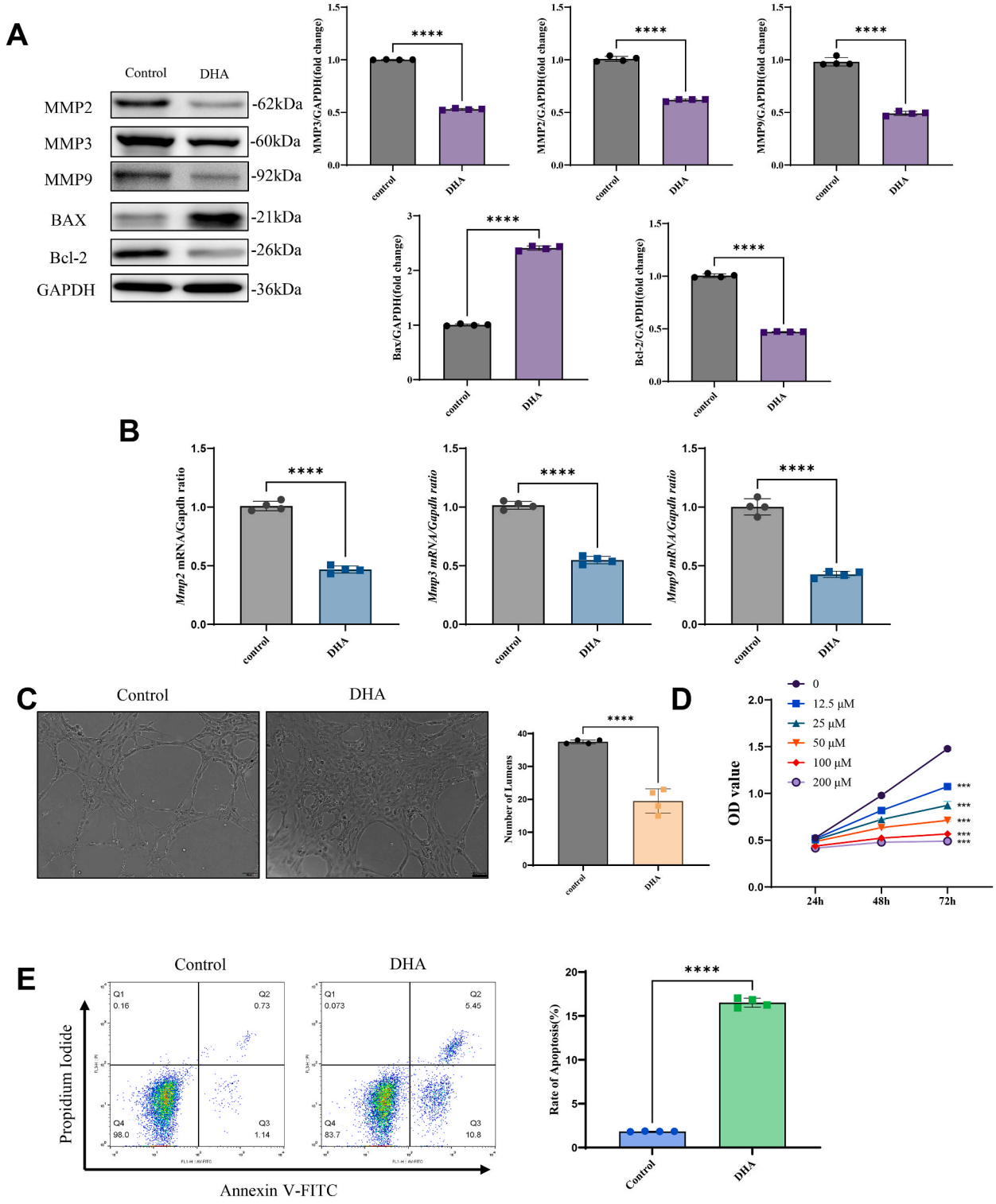

Fig. 1. The expression of EphA2 in BGSCs was downregulated by DHA.
Legend.
A) Results of western blot of MMPs, Bax and BCL-2 and the quantitative analysis. B) The relative expression of Mmp2, Mmp3 and Mmp9 mRNA. C) Results of VM formation of BGSCs with or without 100 μM DHA for 48 h and quantitative analysis.
D) Results of CCK-8 assay of C6 BGSCs after 24-, 48- or 72-h treatment of DHA at different doses(0, 10, 25, 50, 75, 100, 200 μM). E) FACS results of BGSCs with or without 100 μM DHA and quantitative analysis. Bar, 50 μm *$p < 0.05$, ***$p < 0.001$ using student *t*-test. n = 4 for each group.

Fisher Scientific) on a Real-Time PCR machine (Applied Biosystems 7500)and fold changes in gene expression were calculated by the $2^{-\Delta\Delta Ct}$ approach. The primers used in this study were synthesized by Sangon Biotech and Primer Premier 5.0 software and listed in Table 1.

2.10. Orthotopic transplantation mouse model

The animal study was reviewed and approved by the Animal Ethical and Welfare Committee of Guangxi Medical University. Male nude mice of six-week-old BALB/c nude mice were purchased from Charles River company, and raised at the Animal Experimental Center of Guangxi Medical University. To establish an *in vivo* orthotopic transplantation GBM model, C6 cells stably expressing Luciferase (1.5×10^7 cells per mouse) were injected into the striatum of the mice using a 69100 rotary digital stereotaxic apparatus (RWD, Shenzhen, China). Mice were randomly divided into five groups, (namely, Control; DHA; DHA + pc-NC; DHA + pc-EphA2; DHA + pc-EphA2+LY294002, n = 7 per group, DHA [at 100 μM]) and administered daily by gavage. The body weight of the mice was measured. On the 7th, 14th, and 28th day of transplantation, the bioluminescence imaging of tumors was analyzed by a three-dimensional bioluminescence imaging system for small animals (PhotonIMAGER Optima, Biospace Lab, France). All nude mice were sacrificed 28 days after transplantation, and the fluorescence intensity values were analyzed to evaluate the therapeutic effect of DHA on in situ GBM. The brains were collected for HE staining, DAB staining and western blotting detection.

2.11. Statistical analysis

All experiments were performed at least three independent times. Statistical analyses were performed using image J and GraphPad Prism 9.0 software. The statistical analysis significance between multiple groups was performed using analysis of variance (ANONA) and the statistical significance between two means was analyzed by student's t-test. The data were expressed as the means ± standard error of the mean (SEM). Differences with $p < 0.05$ were considered to be statistically significant.

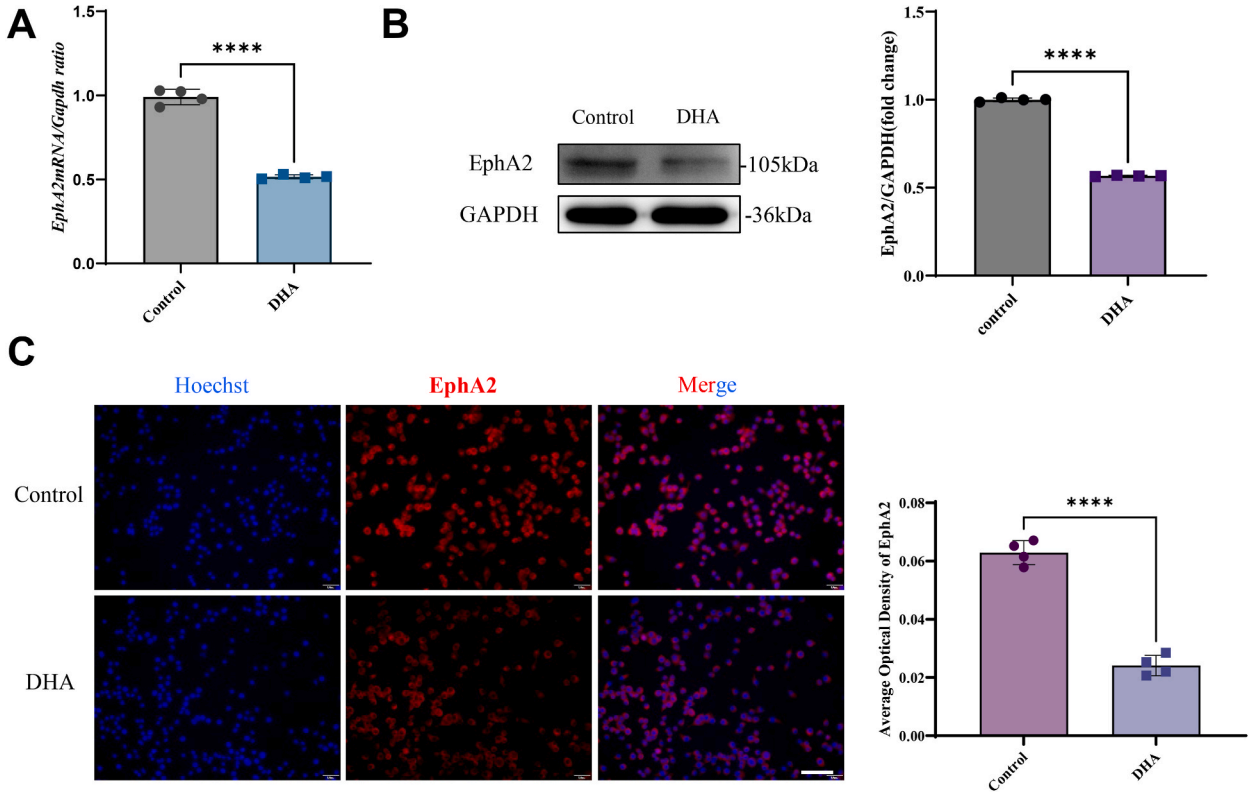

Fig. 2. DHA downregulates EphA2 in brain glioma stem cells.
Legend.
A) The relative expression of Epha2 mRNA. B) The relative expression of EphA2 protein. C) Immunofluorescent staining of EphA2 (red) of C6 BGSCs (nuclei in blue). Bar, 100 μm ***$p < 0.001$ using student *t*-test. $n = 4$ for each group.

3. Results

3.1. The EphA2/MMPs pathway and VM formation in brain glioma stem cells was downregulated by DHA

In this study, BGSCs, characterized by higher expression of CD133 (Supplementary Fig. 1) treated with DHA had a significantly decreased level of EphA2 mRNA and proteins (Fig. 2A and B). The alternation was further confirmed by IF staining (Fig. 2C). The relative expression of MMP-2/3/9, the key downstream mediators of VM formation, were also downregulated in terms of WB (Fig. 2B) and qPCR (Fig. 2A) results. DHA significantly attenuates the VM formation of BGSCs (Fig. 1C). Additionally, the pro-apoptotic protein Bax was increased, while the anti-apoptotic protein Bcl-2 was decreased in BGSCs treated with DHA (Fig. 1A). Decreased cell viability and induced apoptosis, as demonstrated CCK-8 and flow cytometric results further verified the pro-apoptotic effects of DHA (Fig. 1D and E; Supplementary Figs. 2 and 3). Conclusively, these data demonstrated that DHA could inhibit EphA2/MMPs-mediated VM formation and malignant biological behaviors.

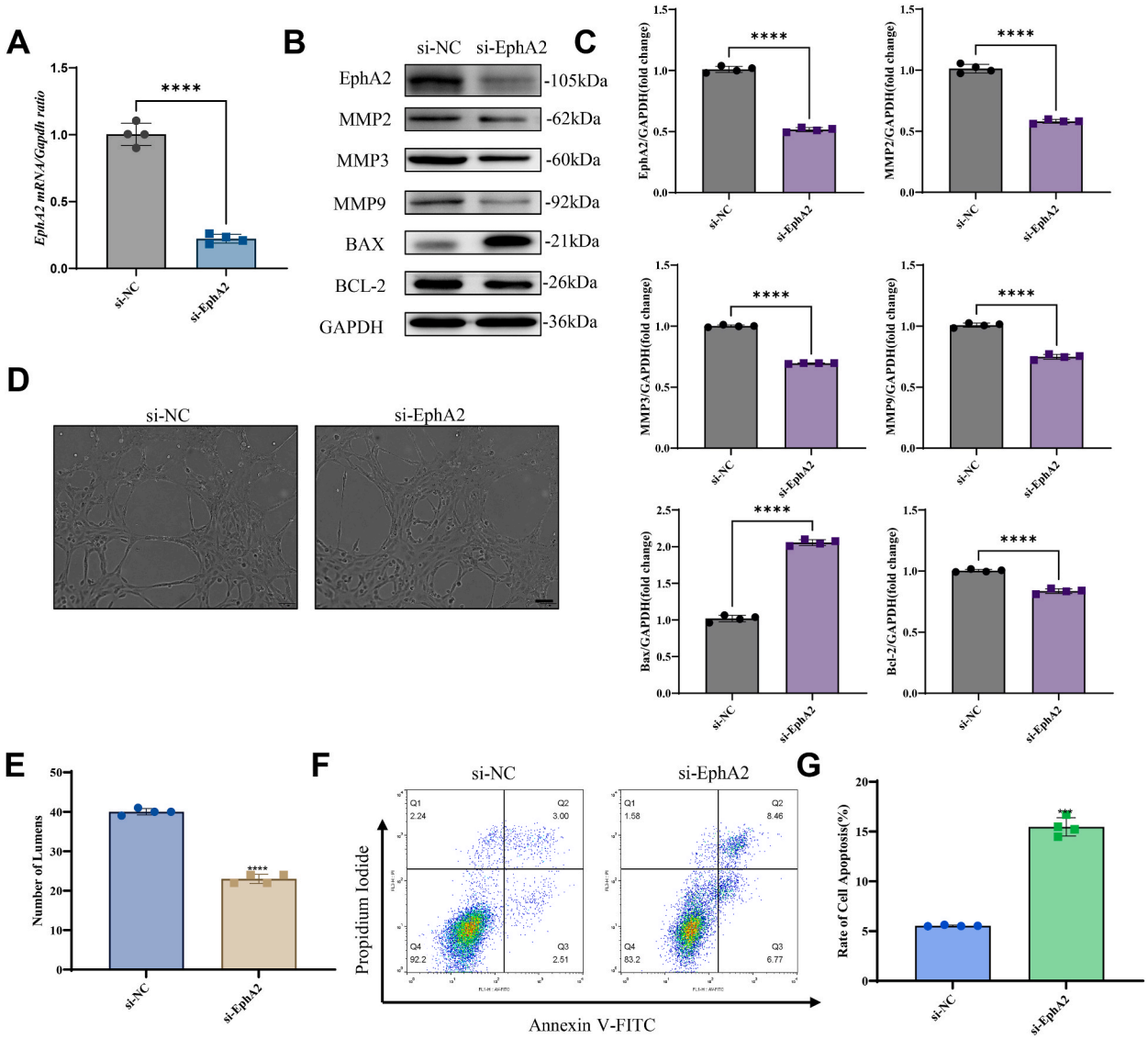

Fig. 3. Knockdown of EphA2 inhibits malignant biological behaviors of brain glioma stem cells.
Legend.
A) The relative expression of Epha2 mRNA between the BGSCs treated with si-NC RNA and si-EphA2 RNA. B,C) Results of western blot of cells treated with si-NC or si-Epha2 and quantitative analysis. D,E) Results of VM formation of BGSCs after EphA2 knockdown and quantitative analysis. F,G) Results of flow cytometry of cells treated with si-NC or si-Epha2 for 72 h. Bar, 50 μm ***$p < 0.001$. ****$p < 0.0001$ using student *t*-test. $n = 4$ for each group.

3.2. The knockdown of EphA2 inhibits VM formation and induces apoptosis in BGSCs

To explore whether the effects of inhibiting VM formation and inducing apoptosis of DHA were mediated by EphA2, small interfering RNA (siRNA) was used to knockdown EphA2 in BGSCs. The mRNA and protein levels of EphA2 were significantly inhibited (Fig. 3AC). IF staining also revealed a significant decrease of EphA2 level (Supplementary Fig. 4). The MMP-2/3/9 were also downregulated after EphA2 knockdown (Fig. 3B and C). Similar to DHA, si-EphA2 also significantly inhibited the formation of VM

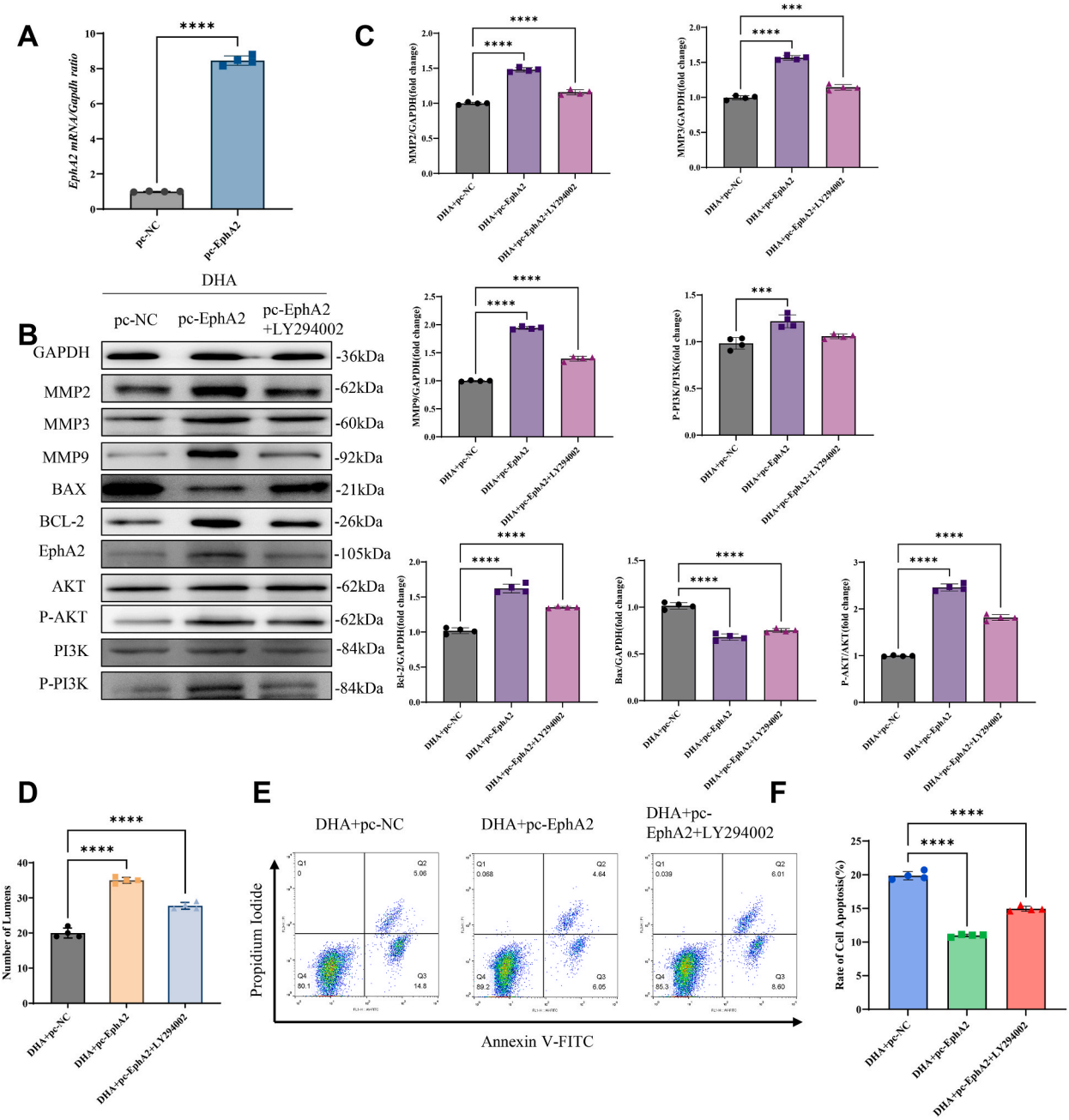

Fig. 4. The anti-glioma effects of DHA was at least partly mediated by downregulation of EphA2.
Legend: A) The relative expression level of EphA2 mRNA after transfection with pcDNA-EphA2. B,C) Western blot results of BGSCs treated with DHA + pc-NC, DHA + pc-EphA2 or DHA + pc-EphA2+LY294002, and quantitative analysis for 48h. D) Results of angiogenesis of BGSCs treated with DHA + pc-NC, DHA + pc-EphA2 or DHA + pc-EphA2+LY294002 for 48h. E,F) Representative images and quantitative analysis of flow cytometric results of Annexin V/PI to identify the ratio of apoptotic cells. *$p < 0.05$, **$p < 0.01$, ***$p < 0.001$, ****$p < 0.0001$ using student *t*-test. $n = 4$_ for each group.

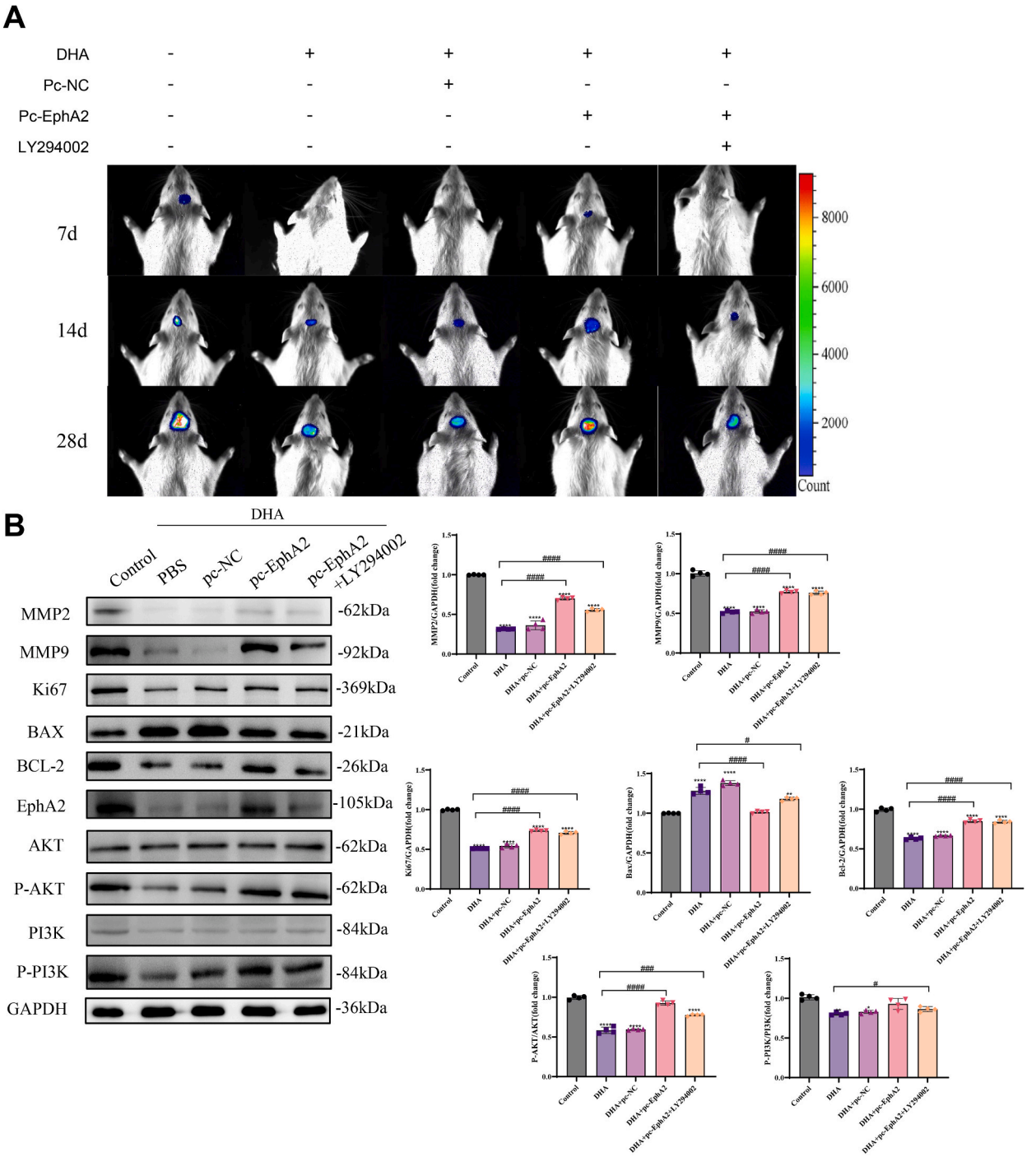

Fig. 5. The anti-glioma effects of DHA were dependent on EphA2/PI3K/MMP inhibition.
Legend.
A) IVIS for glioma tissue after treatment of DHA with or without pc-EphA2 and LY294002 for 48h. B) Western blot results of glioma tissue after treatment of DHA with or without pc-EphA2 and LY294002 for 48h and the quantitative analyses. * or ##$p < 0.05$. ** or ##$p < 0.01$. *** or ###$p < 0.001$. **** or ####$p < 0.0001$ using one-way ANOVA test. $n = 4$ for each group.

(Fig. 3D and E) and induced apoptosis (Fig. 3F and G). These findings indicated that knockdown of EphA2 led to inhibition of VM formation and enhancement of cell apoptosis.

3.3. The anti-glioma effects of DHA were dependent on EphA2/PI3K/MMPs pathway

To investigate whether overexpression of EphA2 rescues the anti-glioma effects of DHA, The expression plasmid of EphA2 (pcDNA-EphA2) and an inhibitor of PI3K signal(LY294002), the downstream of EphA2, were added into the medium of BGSCs. The expression levels of EphA2 mRNA and protein were significantly increased (Fig. 4AC). PI3K and Akt were significantly activated and MMP-2/3/9 were upregulated in EphA2-overexpressed BGSCs (Fig. 4B and C). In BGSCs treated with pcDNA-EphA2 and LY294002, PI3K/Akt/MMPs pathway was significantly inactivated (Fig. 4B and C). The formation of VM increased, and the apoptosis was inhibited in pc-EphA2-treated BGSCs, which were reversed by PI findings indicated that the anti-VM and pro-apoptosis effects of DHA were dependent on EphA2/PI3K/MMPs pathway.

3.4. The anti-glioma effects of DHA in vivo were dependent on EphA2/PI3K/MMPs pathway

To investigate the role of DHA-induced inhibition of EphA2/PI3K/MMPs signal *in vivo*, mice glioma models were established. DHA, pcDNA-EphA2 and LY294002 were administrated in certain groups, as shown in Fig. 5A(Supplementary Fig. 5). Those with DHA + PBS or DHA + pc-NC treatment had significant attenuation of glioma burden, with decreased levels of the activation of PI3K/Akt signal and expression of MMPs (Fig. 5B). The addition of pc-EphA2 reversed the alternations in DHA + PBS or DHA + pc-NC groups; while the growth of glioma was mildly inhibited in the groups treated with DHA + pc-EphA2+LY294002 comparing with the DHA + pc-EphA2 group. Several histological assessments were conducted to understand the mechanisms underlying the relationship between EphA2/PI3K/MMP pathway and DHA-induced anti-glioma effects (Fig. 6A). It was observed that DHA and pc-EphA2 or LY294002 treated inhibited VM formation of $CD31^{-}PAS^{+}$ and promoted the formation of endothelial microvessel(Fig. 6B). The IF staining verified the results of WB regarding the protein levels of EphA2 and MMP-2 in all groups (Fig. 6C and D). Although the key protein levels of WB seemed to be comparable between the DHA + pc-EphA2+LY294002 group and the DHA + pc-EphA2 group, the levels of EphA2 and MMP-2 was decreased according to IF staining. Additionally, the levels of BGSCs in glioma tissues were analyzed by CD133/Nestin staining (Fig. 6A–E), demonstrating the EphA2/PI3K/MMP signal mediates DHA-induced anti-BGSC effects. Conclusively, EphA2/PI3K/MMPs serve as a key pathway mediating the anti-VM and anti-glioma effects of DHA *in vivo*.

4. Discussion

In this study, we revealed that DHA significantly inhibits the formation of vasculogenic-like networks, the stemness of C6 BGSCs and the growth of glioma by inhibiting the expression of EphA2. Mechanistic investigations indicated that the PI3K/Akt pathway at least partly mediates the function, as overexpression of EphA2 reversed the anti-tumor effects of DHA. Conclusively, the current report provides evidence of DHA, PI3K/Akt/EphA2 blockage and VM inhibition as promising therapies for glioma.

Eph receptors are single transmembrane proteins with extracellular-(N-terminal) and intracellular domains with ligand binding and intrinsic enzymatic activities [18]. Some of the Eph receptors, including EphA2 and related ligands (ephrins), have spurred most efforts due to there hypothesized or indicated contribution to carcinogenesis and progression, as they participate in multiple biological processes, mostly causing cell-cell repulsion or adhesion [19,20]. In particular, EphA2 is of great interest due to its capability of directing vascular network assembly, affecting capillary morphogenesis and angiogenesis in addition to regulating the stem properties of BGSCs [21,22]. The expression of EphA2 is at low levels in normal neural tissue and significantly overexpressed in glioma [23].

Malignant glioma is characterized by abnormal angiogenesis, infiltrative growth, and metastasis, leading to incomplete surgical removal and recurrence. Distinct from classical tumor angiogenesis, VM provides a blood supply for tumor cells independent of endothelial cells [24]. Cancer stem cells are crucial modulators in the process of VM formation [25,26]. VM is associated with high tumor grade, invasion, metastasis, and poor prognosis in patients with malignant tumors, and has been considered as a therapeutic target of glioma recently [24]. Downregulating tumor growth factor (TGF) β by RNA interference led to a significantly impaired VM formation, which could be rescued by rhTGFβ in U251MG glioma cells [27]. PP2, a Src tyrosine kinase inhibitor,was also found to downregulate the expression of EphA2 and MMP2, and inhibit VM formation [28]. Similarly, miR-26b and miR-141 also regulate the glioma VM via EphA2 [29,30]. PI3K/Akt/MMP-2/9 signaling was considered another essential pathway mediating EphA2-related VM formation. For instance, in a study focusing on choroidal melanoma, the expression levels of EphA2, PI3K and MMPs and angiogenesis were decreased by curcumin, another natural bioactive molecule, indicating that EphA2/PI3K/MMPs signaling pathway could be a clinical inhibitor of tumor vasculogenic mimicry [31]. Liu et al. showed that miR-451a negatively regulates EphA2 along with the downstream PI3K/Akt pathway, and subsequently the growth and metastasis of bladder cancer cells [32]. In this report, we revealed that EphA2 was downregulated after DHA treatment in glioma stem cells. Similar to bladder and melanoma cells, PI3K, Akt and MMPs were also downregulated following the EphA2 inhibition in BGSCs. However, it remains unclear how DHA inhibits the expression of EphA2, and thus, studies on the upstream or ligands are required. In addition to ephrinA, findings from Gai et al. revealed that EphA2 is also a potential receptor of platelet-derived growth subunit A (PDGFA) and synergetic benefits were observed with simultaneous inhibition of both EphA2 and platelet-derived growth factor receptor α (PDGFRA) in vitro and *in vivo* [33]. It is interesting to note that Hamaoka Y et al. demonstrated that EphA2 is an effector in the downstream of the MEK/ERK/RSK pathway and mediates cell proliferation in glioblastoma cells [34,35], although EphA2 could also regulate MEK/ERK signal [36].

Artemisinin and derivatives, which are derived from the annual Artemisia annua L., have been initially used as anti-malarial agent

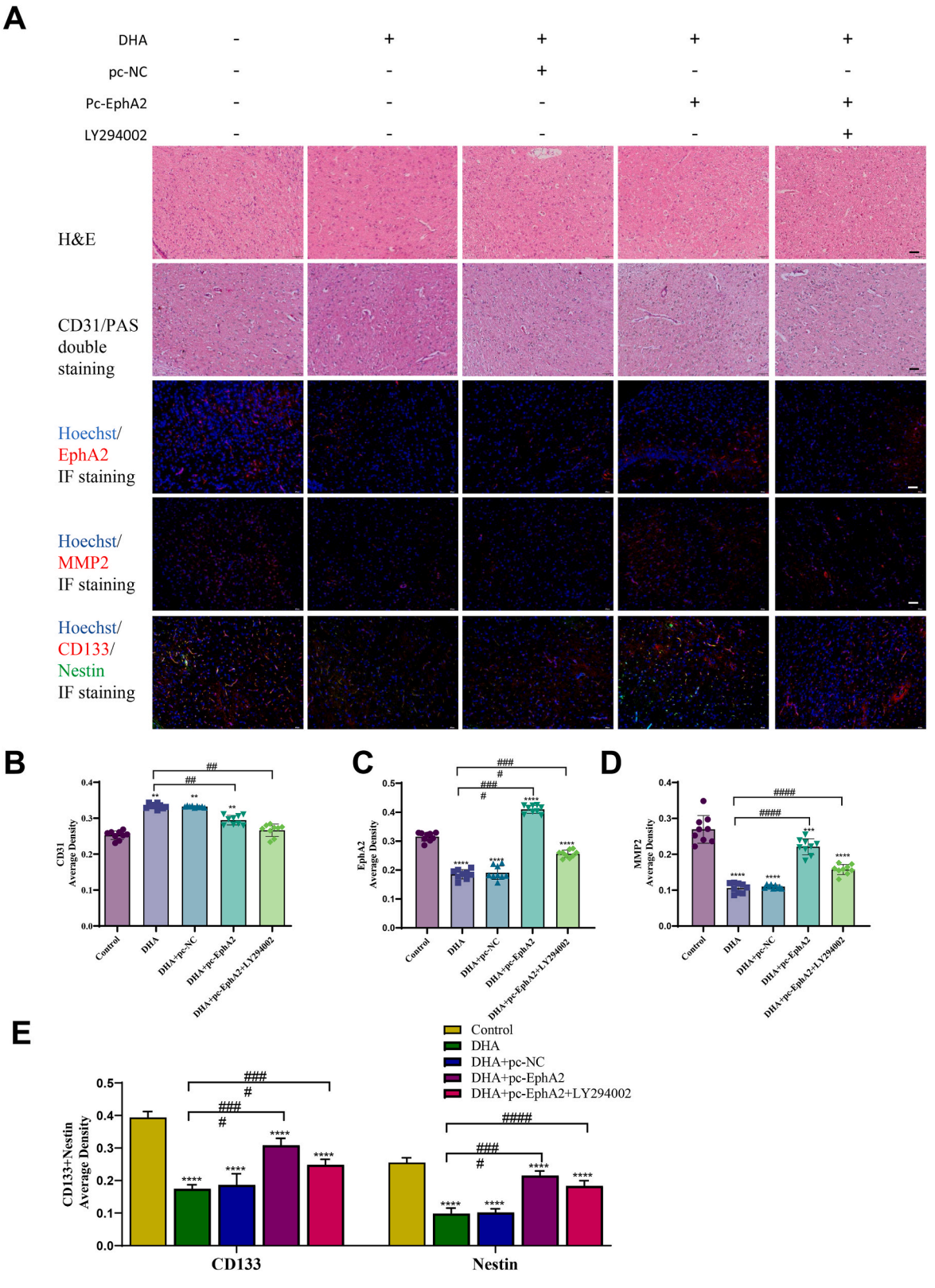

(caption on next page)

Fig. 6. The anti-VM and pro-apoptotic effects of DHA were dependent on EphA2/PI3K/MMP inhibition.
Legend.
A) Histological analysis for glioma tissue after treatment of DHA with or without pc-EphA2 and LY294002 for 48h. B) Quantitative analysis for CD31/PAS double staining. C) Quantitative analysis for EphA2 IF staining. D) Quantitative analysis for MMP2 IF staining. E) Quantitative analysis for CD133/Nestin IF staining. Bar, 50 μm** or $\#\#p < 0.01$. *** or $\#\#\#p < 0.001$. **** or $\#\#\#\#p < 0.0001$ using one-way ANOVA test. $n = 4$ for each group.

for over 2000 years [37]. Recently, DHA has also been recognized as a promising antitumor reagent. DHA efficiently inhibits cell proliferation, induces cell cycle arrest, and promotes apoptosis by regulating Bax, Mcl-1, STAT3, surviving, and other key molecules in several lung cancer cell lines [38–40]. Yao et al. demonstrated that DHA can inactivate cancer-associated fibroblasts by inhibiting the TGFβ signal [41]. Moreover, DHA suppresses the specificity protein 1 and MAPK pathways to inhibit proliferation and induce caspase-dependent apoptosis in SK-Hep-1 cells (a hepatocellular cancer cell line) [42]. In the current study, the anti-glioma effects of DHA were blocked by overexpression of EphA2 using a plasmid, while additional administration of the PI3K inhibitor LY294002 reversed the benefits. These data provide novel mechanistic understanding and preclinical evidence for the administration of DHA and inhibition of EphA2 in the treatment of glioma. Conclusively, DHA significantly inhibits the stemness of BGSCs and VM formation both in vitro and *in vivo*. Mechanistically, the EphA2/PI3K/Akt pathway at least partly mediates the benefits.

CRediT authorship contribution statement

Huangde Fu: Writing – original draft, Formal analysis, Data curation, Conceptualization. **Shengtian Wu:** Formal analysis, Data curation, Conceptualization. **Hechun Shen:** Project administration, Methodology, Investigation, Data curation. **Kai Luo:** Visualization, Validation, Supervision, Software, Resources. **Zhongxiang Huang:** Visualization, Validation, Supervision, Methodology, Conceptualization. **Nankun Lu:** Software, Resources, Project administration, Investigation, Funding acquisition. **Yaolin Li:** Writing – review & editing, Formal analysis, Data curation. **Qian Lan:** Visualization, Investigation. **Yishun Xian:** Writing – review & editing, Visualization, Validation.

Ethical statement

All animal experiments were approved by the Institutional Animal Care and Use Committee of Zhuoqiang Biotechnology,Co.Ltd. (NO. ZQlA-2023-028) and were conducted in accordance with the Guiding Opinions on the Treatment of Laboratory Animals and the Laboratory Animal-Guideline for Ethical Review of Animal Welfare (People's Republic of China national standard GB/T35892-2018).

Data availability statement

The data that support the findings of this study are available within the article. Additional data are available from the corresponding author upon reasonable request.

Funding

This work is supported by Nanning Outstanding Youth Science and Technology Innovation and Entrepreneurship Talent Cultivation Project (RC20210106).

Declaration of competing interest

This manuscript was written by Huangde Fu, Shengtian Wu, Hechun Shen, Kai Luo, Zhongxiang Huang, Nankun Lu, Yaolin Li, Qian Lan, Yishun Xian. All authors have read and approved this version of the article, and due care has been taken to ensure the integrity of the work. This article has never been published previously and not being submitted for publication elsewhere. This paper has no conflicts of interest.

Acknowledgments

None.

Appendix A. Supplementary data

Supplementary data to this article can be found online at https://doi.org/10.1016/j.heliyon.2025.e42095.

References

[1] A. Omuro, L.M. DeAngelis, Glioblastoma and other malignant gliomas: a clinical review, JAMA 310 (17) (2013) 1842–1850.
[2] Q.T. Ostrom, J.S. Barnholtz-Sloan, Current state of our knowledge on brain tumor epidemiology, Curr. Neurol. Neurosci. Rep. 11 (3) (2011) 329–335.
[3] Q. Wang, et al., Tumor Evolution of glioma-intrinsic gene expression subtypes associates with immunological changes in the microenvironment, Cancer Cell 32 (1) (2017) 42–56.e6.
[4] K. Angara, T.F. Borin, A.S. Arbab, Vascular mimicry: a novel neovascularization mechanism driving anti-angiogenic therapy (aat) resistance in glioblastoma, Transl Oncol 10 (4) (2017) 650–660.
[5] A.J. Maniotis, et al., Vascular channel formation by human melanoma cells in vivo and in vitro: vasculogenic mimicry, Am. J. Pathol. 155 (3) (1999) 739–752.
[6] Y. Zhu, et al., Celastrol suppresses glioma vasculogenic mimicry formation and angiogenesis by blocking the PI3K/Akt/mTOR signaling pathway, Front. Pharmacol. 11 (2020) 25.
[7] H. Wang, et al., Vasculogenic mimicry in prostate cancer: the roles of EphA2 and PI3K, J. Cancer 7 (9) (2016) 1114–1124.
[8] E.B. Pasquale, Eph receptors and ephrins in cancer: bidirectional signalling and beyond, Nat. Rev. Cancer 10 (3) (2010) 165–180.
[9] H. Miao, et al., EphA2 mediates ligand-dependent inhibition and ligand-independent promotion of cell migration and invasion via a reciprocal regulatory loop with Akt, Cancer Cell 16 (1) (2009) 9–20.
[10] E. Binda, et al., The EphA2 receptor drives self-renewal and tumorigenicity in stem-like tumor-propagating cells from human glioblastomas, Cancer Cell 22 (6) (2012) 765–780.
[11] Y. Li, Qinghaosu (artemisinin): chemistry and pharmacology, Acta Pharmacol. Sin. 33 (9) (2012) 1141–1146.
[12] Y.J. Mi, et al., Dihydroartemisinin inhibits glucose uptake and cooperates with glycolysis inhibitor to induce apoptosis in non-small cell lung carcinoma cells, PLoS One 10 (3) (2015) e0120426.
[13] N.P. Singh, H. Lai, Selective toxicity of dihydroartemisinin and holotransferrin toward human breast cancer cells, Life Sci. 70 (1) (2001) 49–56.
[14] J.J. Lu, et al., The anti-cancer activity of dihydroartemisinin is associated with induction of iron-dependent endoplasmic reticulum stress in colorectal carcinoma HCT116 cells, Invest. N. Drugs 29 (6) (2011) 1276–1283.
[15] Y. Chen, et al., Dihydroartemisinin-induced unfolded protein response feedback attenuates ferroptosis via PERK/ATF4/HSPA5 pathway in glioma cells, J. Exp. Clin. Cancer Res. 38 (1) (2019) 402.
[16] Z. Que, et al., Dihydroartemisinin inhibits EMT of glioma via gene BASP1 in extrachromosomal DNA, Biochem. Biophys. Res. Commun. 675 (2023) 130–138.
[17] X. Dai, et al., Dihydroartemisinin: a potential natural anticancer drug, Int. J. Biol. Sci. 17 (2) (2021) 603–622.
[18] T. Xiao, et al., Targeting EphA2 in cancer, J. Hematol. Oncol. 13 (1) (2020) 114.
[19] M. Tandon, S.V. Vemula, S.K. Mittal, Emerging strategies for EphA2 receptor targeting for cancer therapeutics, Expert Opin. Ther. Targets 15 (1) (2011) 31–51.
[20] V.C. Dodelet, E.B. Pasquale, Eph receptors and ephrin ligands: embryogenesis to tumorigenesis, Oncogene 19 (49) (2000) 5614–5619.
[21] B.A. McCormick, B.R. Zetter, Adhesive interactions in angiogenesis and metastasis, Pharmacol. Ther. 53 (2) (1992) 239–260.
[22] E. Stein, et al., Eph receptors discriminate specific ligand oligomers to determine alternative signaling complexes, attachment, and assembly responses, Genes Dev. 12 (5) (1998) 667–678.
[23] Q. Wu, et al., MicroRNA-124-3p represses cell growth and cell motility by targeting EphA2 in glioma, Biochem. Biophys. Res. Commun. 503 (4) (2018) 2436–2442.
[24] Q. Luo, et al., Vasculogenic mimicry in carcinogenesis and clinical applications, J. Hematol. Oncol. 13 (1) (2020) 19.
[25] B. Sun, et al., Epithelial-to-endothelial transition and cancer stem cells: two cornerstones of vasculogenic mimicry in malignant tumors, Oncotarget 8 (18) (2017) 30502–30510.
[26] Y. Izawa, et al., Stem-like human breast cancer cells initiate vasculogenic mimicry on matrigel, Acta Histochem. Cytoc. 51 (6) (2018) 173–183.
[27] G. Ling, et al., Transforming growth factor-β is required for vasculogenic mimicry formation in glioma cell line U251MG, Cancer Biol. Ther. 12 (11) (2011) 978–988.
[28] K.Y. Eom, et al., The effect of chemoradiotherapy with SRC tyrosine kinase inhibitor, PP2 and temozolomide on malignant glioma cells in vitro and in vivo, Cancer Res Treat 48 (2) (2016) 687–697.
[29] G. Li, et al., miR-141 inhibits glioma vasculogenic mimicry by controlling EphA2 expression, Mol. Med. Rep. 18 (2) (2018) 1395–1404.
[30] N. Wu, et al., Role of microRNA-26b in glioma development and its mediated regulation on EphA2, PLoS One 6 (1) (2011) e16264.
[31] L.X. Chen, et al., Inhibition of tumor growth and vasculogenic mimicry by curcumin through down-regulation of the EphA2/PI3K/MMP pathway in a murine choroidal melanoma model, Cancer Biol. Ther. 11 (2) (2011) 229–235.
[32] B. Liu, et al., microRNA-451a promoter methylation regulated by DNMT3B expedites bladder cancer development via the EPHA2/PI3K/AKT axis, BMC Cancer 20 (1) (2020) 1019.
[33] Q.J. Gai, et al., EPHA2 mediates PDGFA activity and functions together with PDGFRA as prognostic marker and therapeutic target in glioblastoma, Signal Transduct. Targeted Ther. 7 (1) (2022) 33.
[34] Y. Hamaoka, M. Negishi, H. Katoh, EphA2 is a key effector of the MEK/ERK/RSK pathway regulating glioblastoma cell proliferation, Cell. Signal. 28 (8) (2016) 937–945.
[35] P.R. Graves, et al., Ionizing radiation induces EphA2 S897 phosphorylation in a MEK/ERK/RSK-dependent manner, Int. J. Radiat. Biol. 93 (9) (2017) 929–936.
[36] Y. Kaibori, Y. Saito, Y. Nakayama, EphA2 phosphorylation at Ser897 by the Cdk1/MEK/ERK/RSK pathway regulates M-phase progression via maintenance of cortical rigidity, Faseb. J. 33 (4) (2019) 5334–5349.
[37] D.L. Klayman, Qinghaosu (artemisinin): an antimalarial drug from China, Science 228 (4703) (1985) 1049–1055.
[38] D. Mu, et al., The role of calcium, P38 MAPK in dihydroartemisinin-induced apoptosis of lung cancer PC-14 cells, Cancer Chemother. Pharmacol. 61 (4) (2008) 639–645.
[39] Q. Sun, et al., Enhanced apoptotic effects of dihydroartemisinin-aggregated gelatin and hyaluronan nanoparticles on human lung cancer cells, J. Biomed. Mater. Res. B Appl. Biomater. 102 (3) (2014) 455–462.
[40] X. Yan, et al., Dihydroartemisinin suppresses STAT3 signaling and Mcl-1 and Survivin expression to potentiate ABT-263-induced apoptosis in Non-small Cell Lung Cancer cells harboring EGFR or RAS mutation, Biochem. Pharmacol. 150 (2018) 72–85.
[41] Y. Yao, et al., Artemisinin derivatives inactivate cancer-associated fibroblasts through suppressing TGF-β signaling in breast cancer, J. Exp. Clin. Cancer Res. 37 (1) (2018) 282.
[42] E. Im, et al., Dihydroartemisinin induced caspase-dependent apoptosis through inhibiting the specificity protein 1 pathway in hepatocellular carcinoma SK-Hep-1 cells, Life Sci. 192 (2018) 286–292.